



Title	Extended optimal Fermi averaging for near-recoilless production in the (K - , - ) reaction on nuclei
Author(s)	Harada, Toru; Hirabayashi, Yoshiharu
Citation	Physical Review C, 105(6), 64606 <a href="https://doi.org/10.1103/PhysRevC.105.064606">https://doi.org/10.1103/PhysRevC.105.064606</a>
Issue Date	2022
Doc URL	<a href="http://hdl.handle.net/2115/86573">http://hdl.handle.net/2115/86573</a>
Rights	©2022 American Physical Society
Type	article
File Information	PhysRevC.105.064606.pdf



[Instructions for use](#)

## Extended optimal Fermi averaging for near-recoilless $\Lambda$ production in the $(K^-, \pi^-)$ reaction on nuclei

Toru Harada<sup>1,2,\*</sup> and Yoshiharu Hirabayashi<sup>3</sup>

<sup>1</sup>*Center for Physics and Mathematics, Osaka Electro-Communication University, Neyagawa, Osaka 572-8530, Japan*

<sup>2</sup>*J-PARC Branch, KEK Theory Center, Institute of Particle and Nuclear Studies,*

*High Energy Accelerator Research Organization (KEK), 203-1, Shirakata, Tokai, Ibaraki 319-1106, Japan*

<sup>3</sup>*Information Initiative Center, Hokkaido University, Sapporo 060-0811, Japan*



(Received 9 March 2022; revised 9 May 2022; accepted 3 June 2022; published 15 June 2022)

We propose to extend the optimal Fermi averaging procedure theoretically in order to calculate an in-medium  $K^-n \rightarrow \pi^- \Lambda$  amplitude for the exothermic  $(K^-, \pi^-)$  reaction on nuclei in the framework of a distorted-wave impulse approximation, taking into account the local momentum transfer generated by semiclassical distorted waves for  $K^-$  and  $\pi^-$  mesons. Angular distributions for the  $^{12}\text{C}(K^-, \pi^-)_{\Lambda}^{12}\text{C}$  reaction in which a momentum transfer is  $q \lesssim 80$  MeV/c at  $p_K = 800$  MeV/c in the  $\pi^-$  forward direction are estimated by applying the extended procedure. The result shows that the calculated angular distributions are in good agreement with those of the data, and this extension is a successful prescription making it possible to describe the reaction cross sections in near-recoilless reactions such as  $(K^-, \pi^-)$  in our framework.

DOI: [10.1103/PhysRevC.105.064606](https://doi.org/10.1103/PhysRevC.105.064606)

### I. INTRODUCTION

The  $(K^-, \pi^-)$  reaction has been an essential tool for studying spectroscopy in hypernuclear physics and strange particle physics [1–3]. This reaction has played an important role in understanding hypernuclear structures related to the nature of  $YN$  interaction, by controlling a momentum transfer over a wide range of  $q = 0$  to a few hundred MeV/c in the exothermic reaction [4,5], in comparison with endothermic reactions such as  $(\pi^+, K^+)$  and  $(e, e'K^+)$  having large momentum transfers of  $q \simeq 300$ –500 MeV/c.

Several authors [6–10] studied a shell-model approach to  $\Lambda$  hypernuclear spectroscopy in  $p$ -shell nuclei within a distorted-wave impulse approximation (DWIA), considering a Fermi averaging of a  $K^-n \rightarrow \pi^- \Lambda$  amplitude, recoil corrections, and distorted waves obtained by solving the Klein-Gordon equations for  $K^-$  and  $\pi^-$  mesons. The Fermi averaging treatment [11] may essentially affect the shape and magnitude of the production cross sections in the  $K^-n \rightarrow \pi^- \Lambda$  reaction on nuclei because there appear narrow  $Y^*$  resonances whose widths are smaller than the Fermi-motion energy of a struck nucleon in the nuclei [7]. These studies extract valuable information on the structure of hypernuclear states and the mechanism of hyperon production reactions from available experimental data at CERN, BNL, and KEK. The experimental studies are now in progress at J-PARC [12].

However, the authors [13–15] showed that the energy and angular dependence of an in-medium amplitude of  $\bar{f}_{\pi^- p \rightarrow K^+ \Sigma^-}$  is significant to explain the behavior of  $\Sigma^-$  production spectra for nuclear  $(\pi^-, K^+)$  reactions in the DWIA,

using the optimal Fermi averaging (OFA) procedure [16], which provides the Fermi motion of a nucleon on the on-energy-shell  $\pi^- p \rightarrow K^+ \Sigma^-$  reaction condition in a nucleus. This procedure was also applied to  $\Lambda$  production via the  $(\pi^+, K^+)$  reaction [16] and  $\Xi^-$  production via the  $(K^-, K^+)$  on nuclei [17], and indicated a successful description for the  $K^+$  spectra of the data. Therefore, it seems that our OFA procedure works very well for these endothermic reactions characterized by large momentum transfers of  $q \gtrsim 300$ –500 MeV/c.

Kohno and his collaborators [18,19] also discussed the inclusive  $K^+$  spectra via nuclear  $(\pi^\pm, K^+)$  and  $(K^-, K^+)$  reactions using the semiclassical distorted-wave (SCDW) model [20]. Considering the semiclassical approximation [21], Luo and Kawai [20] showed a successful description of  $(p, p'x)$  and  $(p, nx)$  inclusive cross sections for intermediate energy nucleon reactions by the SCDW model.

When we attempt to apply the OFA procedure to a calculation for exothermic  $\Lambda$  production reactions such as  $(K^-, \pi^-)$  on nuclei, however, we realize an unavoidable difficulty that no  $\Lambda$  hyperon is populated in hypernuclear states under a near-recoilless environment, e.g.,  $q \lesssim 80$  MeV/c, contrary to the evidence of experimental observations [1–3]. In the OFA procedure, the on-energy-shell equation [see Eq. (10)] needs to satisfy approximately the condition as a discriminant,

$$\frac{q^2}{2\Delta m} - \Delta\omega \geq 0, \quad (1)$$

with  $\Delta\omega = \varepsilon_\Lambda(j_\Lambda) - \varepsilon_N(j_N)$  and  $\Delta m = m_\Lambda - m_N$ , where  $\varepsilon_\Lambda(j_\Lambda)$  and  $\varepsilon_N(j_N)$  ( $m_\Lambda$  and  $m_N$ ) are energies of the single-particle states (masses) for  $\Lambda$  and  $N$ , respectively. Considering the  $^{12}\text{C}(K^-, \pi^-)_{\Lambda}^{12}\text{C}$  reaction at  $p_K = 800$  MeV/c in the  $\pi^-$  forward direction, we perhaps have difficulty of

\*harada@osakac.ac.jp

$q^2/2\Delta m < \Delta\omega$  due to  $q \lesssim 80$  MeV/c. This conjecture implies that the OFA procedure is not applicable in describing the angular distributions of  $d\sigma/d\Omega_{\text{lab}}$  in this near-recoilless ( $K^-$ ,  $\pi^-$ ) reaction.

In this paper, we propose to extend the OFA procedure [16] theoretically in order to calculate an in-medium  $K^-n \rightarrow \pi^- \Lambda$  amplitude of  $\bar{f}_{K^-n \rightarrow \pi^- \Lambda}$  for the exothermic ( $K^-$ ,  $\pi^-$ ) reaction on nuclei in the framework of the DWIA, taking into account the local momentum transfer generated by semiclassical distorted waves for  $K^-$  and  $\pi^-$  [21]. Applying the extended OFA in the DWIA, we estimate the angular distributions of  $d\sigma/d\Omega_{\text{lab}}$  for the  $^{12}\text{C}(K^-, \pi^-)^{12}\text{C}$  reaction at  $p_K = 800$  MeV/c, in comparison with those obtained in other standard DWIA calculations.

## II. PROCEDURE AND FORMULAS

### A. Distorted-wave impulse approximation

We briefly mention a formulation of the angular distributions for the nuclear ( $K^-$ ,  $\pi^-$ ) reaction in the DWIA. Considering only the non-spin-flip processes in this reaction, the differential cross section for the  $\Lambda$  bound state with a spin parity  $J^P$  at the  $\pi^-$  forward direction angle of  $\theta_{\text{lab}}$  is often written in the DWIA [7,22,23] as (in units  $\hbar = c = 1$ )

$$\left(\frac{d\sigma}{d\Omega}\right)_{\text{lab}}^{J^P} = \alpha \frac{1}{2J_A + 1} \sum_{m_A m_B} |\langle \Psi_B | \bar{f}_{K^-n \rightarrow \pi^- \Lambda} \times \chi_b^{(-)*}(\mathbf{p}_\pi, \mathbf{r}) \chi_a^{(+)}(\mathbf{p}_K, \mathbf{r}) | \Psi_A \rangle|^2, \quad (2)$$

where  $\Psi_B$  and  $\Psi_A$  are wave functions of the hypernuclear final state and the initial state of the target nucleus, respectively.  $\chi_b^{(-)}$  and  $\chi_a^{(+)}$  are distorted waves for outgoing  $\pi^-$  and incoming  $K^-$  mesons, respectively. The kinematical factor  $\alpha$  denotes the translation from a two-body  $K^-$ -nucleon laboratory system to a  $K^-$ -nucleus laboratory system [24]. The energy and momentum transfers to the final state are given by

$$\omega = E_K - E_\pi, \quad \mathbf{q} = \mathbf{p}_K - \mathbf{p}_\pi, \quad (3)$$

where  $E_K = (\mathbf{p}_K^2 + m_K^2)^{1/2}$  and  $E_\pi = (\mathbf{p}_\pi^2 + m_\pi^2)^{1/2}$  ( $\mathbf{p}_K$  and  $\mathbf{p}_\pi$ ) are laboratory energies (momenta) of  $K^-$  and  $\pi^-$  in this reaction, respectively;  $m_K$  and  $m_\pi$  are masses of  $K^-$  and  $\pi^-$ , respectively. The quantity  $\bar{f}_{K^-n \rightarrow \pi^- \Lambda}$  denotes the in-medium  $K^-n \rightarrow \pi^- \Lambda$  non-spin-flip amplitude. An in-medium  $K^-n \rightarrow \pi^- \Lambda$  spin-flip amplitude  $\bar{g}_{K^-n \rightarrow \pi^- \Lambda}$  is neglected in this work because the spin-flip part of the elementary  $K^-n \rightarrow \pi^- \Lambda$  amplitude gives negligible contributions near the forward direction in the ( $K^-$ ,  $\pi^-$ ) reaction [7].

### B. Local momentum transfer

In the semiclassical approximation [21], the *local* momentum transfer in the nucleus may be defined as

$$\begin{aligned} \mathbf{q}(\mathbf{r}) &\equiv \frac{\text{Re}\{(-i\nabla)\chi_b^{(-)*}(\mathbf{p}_\pi, \mathbf{r})\chi_a^{(+)}(\mathbf{p}_K, \mathbf{r})\}}{|\chi_b^{(-)*}(\mathbf{p}_\pi, \mathbf{r})\chi_a^{(+)}(\mathbf{p}_K, \mathbf{r})|} \\ &= \mathbf{p}_K(\mathbf{r}) - \mathbf{p}_\pi(\mathbf{r}), \end{aligned} \quad (4)$$

where  $\mathbf{p}_K(\mathbf{r})$  and  $\mathbf{p}_\pi(\mathbf{r})$  are *local* momenta for  $K^-$  and  $\pi^-$ , respectively, which are generated by the semiclassical

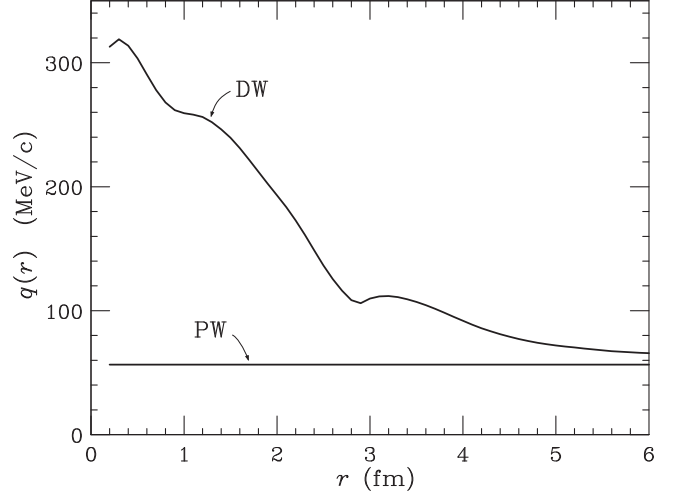


FIG. 1. Magnitude of the local momentum transfers  $q(r)$  for the  $^{12}\text{C}(K^-, \pi^-)^{12}\text{C}$  reaction at the incident  $K^-$  momentum of  $p_K = 800$  MeV/c and  $\theta_{\text{lab}} = 0^\circ$ . The calculated values of the distorted waves (DW) and the plane wave (PW) for the mesons are shown, as a function of the relative distance  $r$  between the mesons and the center of the nucleus. The asymptotic momentum transfer corresponds to  $q_{K\pi} = 56.5$  MeV/c.

distorted waves of  $\chi_a^{(+)}$  and  $\chi_b^{(-)}$  that are assumed to behave as a slowly varying function of a local point  $\mathbf{r}$  in the trajectory. We obtain these distorted waves numerically in program PIRK [25], solving the Klein-Gordon equations for the  $K^-$  and  $\pi^-$  mesons with the standard Kisslinger optical potentials,

$$2EU(r) = -p^2 b_0 \rho_A(r) + b_1 \nabla \cdot \rho_A(r) \nabla, \quad (5)$$

where  $\rho_A(r)$  is the nuclear density normalized to the total number of nucleons,  $A$ . Considering the ( $K^-$ ,  $\pi^-$ ) reaction on  $^{12}\text{C}$  at  $p_K = 800$  MeV/c, we have  $p_\pi = 732$  MeV/c for the  $[(0s_{1/2})_\Lambda(0p_{3/2})_n^{-1}]_{1-}$  state and  $p_\pi = 744$  MeV/c for the  $[(0p_{3/2})_\Lambda(0p_{3/2})_n^{-1}]_{0^+, 2^+}$  states in  $^{12}\text{C}$ . For  $K^-$ , we determine the parameters of  $b_0$  and  $b_1$  in Eq. (5), fitting to the data of the 800-MeV/c scattering on  $^{12}\text{C}$  [26], leading to  $b_0 = 0.309 + i0.498$  fm<sup>3</sup> and  $b_1 = 0$  fm<sup>3</sup> at  $p_K = 800$  MeV/c. For  $\pi^-$  at  $p_\pi = 732$  and 744 MeV/c, we interpolate the values of  $b_0$  and  $b_1$  from the corresponding parameters determined by fits to the data of the 710- and 790-MeV/c scatterings on  $^{12}\text{C}$  [27]; we have  $b_0 = (-0.099 + i0.202)$  fm<sup>3</sup> and  $b_1 = (-0.258 + i0.736)$  fm<sup>3</sup> at  $p_\pi = 732$  MeV/c, and  $b_0 = (-0.095 + i0.201)$  fm<sup>3</sup> and  $b_1 = (-0.228 + i0.736)$  fm<sup>3</sup> at  $p_\pi = 744$  MeV/c.

Figure 1 shows the calculated values of the magnitude of the local momentum transfer  $q(r) = |\mathbf{q}(r)|$  for the  $^{12}\text{C}(K^-, \pi^-)^{12}\text{C}$  reaction at  $p_K = 800$  MeV/c, as a function of the relative distance  $r$  between the mesons and the center of the nucleus. We find that the value of  $q(r)$  amounts to about 300 MeV/c at the nuclear center, and decreases toward the nuclear surface of  $R = r_0 A^{1/3} = 2.91$  fm for  $^{12}\text{C}$ ; it becomes asymptotically  $q_{K\pi} = |\mathbf{p}_K - \mathbf{p}_\pi|$  at  $|\mathbf{r}| \rightarrow \infty$  outside the nucleus, where  $q_{K\pi}$  is an asymptotic momentum transfer corresponding to  $q$  given in Eq. (3). This behavior is determined by the attractive (repulsive) nature of the potential used for

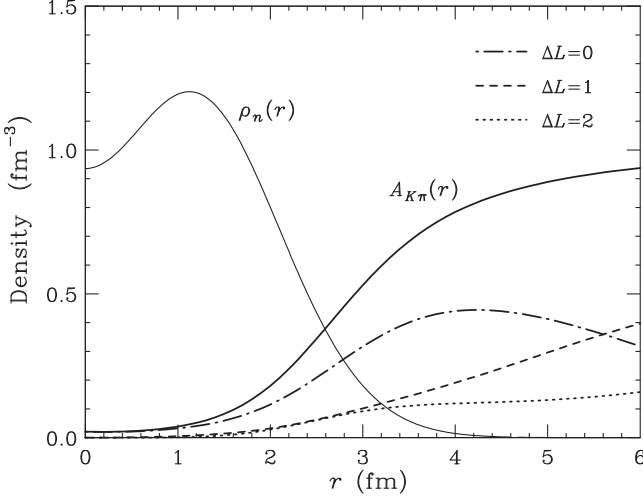


FIG. 2. Meson absorption factor  $A_{K\pi}(r)$  in the  $^{12}\text{C}(K^-, \pi^-)^{12}\text{C}$  reaction at the incident  $K^-$  momentum of  $p_K = 800$  MeV/c and  $\theta_{\text{lab}} = 0^\circ$ , as a function of the relative distance  $r$ . Dot-dashed, dashed, and dotted curves denote the components of the angular momentum transfers with  $\Delta L = 0, 1$ , and  $2$ , respectively. The distribution of the neutron density  $\rho_n(r)$  in  $^{12}\text{C}$  is also drawn.

$K^-$  ( $\pi^-$ ) in Eq. (5). In the plane-wave (PW) approximation for the meson waves, the value of  $q(r)$  is equal to  $q_{K\pi}$  as a constant. To see clearly the effect of the local momentum transfer in the nucleus, we estimate the root-mean-square value of  $q$  defined as

$$\langle q^2 \rangle^{1/2} = \left[ \frac{\int_0^\infty dr r^2 \rho_n(r) A_{K\pi}(r) |q(r)|^2}{\int_0^\infty dr r^2 \rho_n(r) A_{K\pi}(r)} \right]^{1/2}, \quad (6)$$

where  $\rho_n(r)$  is the neutron density in the target nucleus, normalized by  $\int \rho_n(r) d\mathbf{r} = N$ , and  $A_{K\pi}(r)$  is a meson absorption factor [23,28], which is given by

$$A_{K\pi}(r) = \frac{1}{4\pi} \int |\chi_b^{(-)*}(\mathbf{p}_\pi, \mathbf{r}) \chi_a^{(+)}(\mathbf{p}_K, \mathbf{r})|^2 d\Omega. \quad (7)$$

Figure 2 shows the neutron density  $\rho_n(r)$  in  $^{12}\text{C}$  and the absorption factor  $A_{K\pi}(r)$ , as a function of the radial distance. We use a modified harmonic oscillator model with the parameters of  $\alpha = 2.234$  and  $b = 1.516$  fm for  $^{12}\text{C}$  [29], and the distorted waves obtained by Eq. (5). Because the asymptotic momentum transfer is small for the near-recoilless ( $K^-$ ,  $\pi^-$ ) reaction, the partial waves of the angular momentum transfer  $\Delta L \lesssim 2$  in  $A_{K\pi}(r)$  contribute to the  $\Lambda$  production; the component of  $\Delta L = 0$  is dominant inside the nucleus, whereas the components of  $\Delta L = 1$  and  $2$  grow toward the outside of the nucleus. We find  $\langle q^2 \rangle^{1/2} = 203$  MeV/c at  $\theta_{\text{lab}} = 0^\circ$ , of which the value is sufficiently larger than  $q_{K\pi} = 56.5$  MeV/c. The value of  $\langle q^2 \rangle^{1/2}$  may effectively indicate the momentum transfer in the nucleus. Therefore, the local momentum transfer generated by the distorted waves is expected to significantly influence the  $\Lambda$  production cross section for the near-recoilless ( $K^-$ ,  $\pi^-$ ) reaction.

### C. Extended optimal Fermi averaging

Following the semiclassical approximation in Ref. [21], we attempt to extend the OFA procedure [16] for the in-medium  $K^-n \rightarrow \pi^- \Lambda$  amplitude of  $\bar{f}_{K^-n \rightarrow \pi^- \Lambda}$ , taking into account the effect of the local momentum transfer. The extended optimal Fermi-averaged  $K^-n \rightarrow \pi^- \Lambda$   $t$  matrix in the nucleus can be defined as

$$\overline{t^{\text{opt}}}(p_K; \omega, \mathbf{q}) = \frac{\int_0^\infty dr r^2 \rho_n(r) A_{K\pi}(r) t^{\text{opt}}(p_K; \omega, \mathbf{q}(r))}{\int_0^\infty dr r^2 \rho_n(r) A_{K\pi}(r)}, \quad (8)$$

where  $t^{\text{opt}}(p_K; \omega, \mathbf{q})$  is the optimal Fermi-averaged  $K^-n \rightarrow \pi^- \Lambda$   $t$  matrix at a point of  $(\omega, \mathbf{q})$  [16], which is given by

$$t^{\text{opt}}(p_K; \omega, \mathbf{q}) = \frac{\int_0^\pi \sin \theta_N d\theta_N \int_0^\infty dp_N p_N^2 n(p_N) t(E_2; \mathbf{p}_K, \mathbf{p}_N)}{\int_0^\pi \sin \theta_N d\theta_N \int_0^\infty dp_N p_N^2 n(p_N)} \Bigg|_{\mathbf{p}_N = \mathbf{p}_N^*} \quad (9)$$

where  $t(E_2; \mathbf{p}_K, \mathbf{p}_N)$  is the two-body on-shell  $t$  matrix for the  $K^-n \rightarrow \pi^- \Lambda$  reaction in free space,  $E_2 = E_K + E_N$  is a total energy of the  $K^-N$  system, and  $\cos \theta_N = \hat{\mathbf{p}}_K \cdot \hat{\mathbf{p}}_N$ ;  $E_N$  and  $\mathbf{p}_N$  are an energy and a momentum of the nucleon in the nucleus, respectively. The function  $n(p)$  is a momentum distribution of a struck nucleon in the nucleus, normalized by  $\int n(p) d\mathbf{p} / (2\pi)^3 = 1$ ; we estimate  $\langle p^2 \rangle^{1/2} \simeq 147$  MeV/c, assuming a harmonic oscillator model with a size parameter  $b_N = 1.64$  fm for  $^{12}\text{C}$ . The subscript  $\mathbf{p} = \mathbf{p}^*$  in Eq. (9) means the integral with a constraint imposed on the values of  $(p_N, \theta_N)$  that fulfill the condition for  $(p_N, \theta_N) = (p_N^*, \theta_N^*)$  in an on-energy-shell momentum  $\mathbf{p}_N^*$ . The momentum  $\mathbf{p}_N^*$  is a solution that satisfies the on-energy-shell equation for a struck nucleon at the point  $(\omega, \mathbf{q})$  in the nuclear systems,

$$\sqrt{(\mathbf{p}_N^* + \mathbf{q})^2 + m_\Lambda^2} - \sqrt{(\mathbf{p}_N^*)^2 + m_N^2} = \omega, \quad (10)$$

where  $m_\Lambda$  and  $m_N$  are masses of the  $\Lambda$  and the nucleon, respectively. Note that this procedure keeps the on-energy-shell  $K^-n \rightarrow \pi^- \Lambda$  processes in the nucleus [30], so that it guarantees to take ‘‘optimal’’ values for  $t^{\text{opt}}$ ; binding effects for the nucleon and the  $\Lambda$  in the nucleus are considered automatically when we input experimental values for the binding energies of the nuclear and hypernuclear states.

According to the optimal momentum approximation [30], the use of the on-shell  $K^-n \rightarrow \pi^- \Lambda$   $t$  matrix may be valid in the impulse approximation because the leading-order correction caused by the Fermi motion is minimized. Therefore, the OFA procedure is a straightforward way of dealing with the Fermi averaging for the elementary reaction amplitude in the optimal momentum approximation. Moreover, this extension in this work provides the effect of the local momentum transfers in the semiclassical approximation that meson-baryon collisions are spatially localized at a point in the nucleus without interfering with the collisions at different points [21]. By using the extended optimal Fermi-averaged  $t$  matrix in Eq. (8), thus, the in-medium  $K^-n \rightarrow \pi^- \Lambda$  amplitude for the

nucleus in Eq. (2) is given as

$$\bar{f}_{K^-n \rightarrow \pi^- \Lambda} = -\frac{1}{2\pi} \left( \frac{p_\pi E_\pi E_K}{\alpha p_K} \right)^{1/2} t^{\text{opt}}(p_K; \omega, \mathbf{q}), \quad (11)$$

as a function of the incident  $K^-$  momentum  $p_K$  and the detected  $\pi^-$  angle  $\theta_{\text{lab}}$  and momentum  $p_\pi$  in the laboratory frame.

The on-energy-shell equation of Eq. (10) has a solution of  $\mathbf{p}_N^*$  under the condition of  $q^2/2\Delta m > \Delta\omega$  in Eq. (1). Considering the  $^{12}\text{C}(K^-, \pi^-)_{\Lambda}^{12}\text{C}$  reaction, we have  $\Delta m = 1115 - 940 \simeq 175$  MeV,  $\Delta\omega = \varepsilon_\Lambda(0p_{3/2}) - \varepsilon_N(0p_{3/2}) \simeq -1 - (-19) = 18$  MeV for  $0^+$  and  $2^+_{1,2}$  excited states (exc.), and  $\Delta\omega = \varepsilon_\Lambda(0s_{1/2}) - \varepsilon_N(0p_{3/2}) \simeq -11 - (-19) = 8$  MeV for a  $1^-$  ground state (g.s.). When  $q < 80$  MeV/c, it is impossible to populate a  $\Lambda$  in the  $(0p_{3/2})_\Lambda$  states in the framework of the OFA due to  $q^2/2\Delta m < \Delta\omega$ . When  $q < 53$  MeV/c, it is also impossible to populate a  $\Lambda$  in the  $(0s_{1/2})_\Lambda$  state due to  $q^2/2\Delta m < \Delta\omega$ . Therefore, we expect that the extended OFA procedure will overcome the difficulty of  $q^2/2\Delta m < \Delta\omega$  even if the near-recoilless reaction has  $q \lesssim 80$  MeV/c. However, we believe that the standard Fermi averaging (SFA) [7,11] supplies the in-medium amplitude of  $\bar{f}_{K^-n \rightarrow \pi^- \Lambda}$  by an assumption of the off-energy-shell components in the nuclear ( $K^-, \pi^-$ ) reaction condition.

### III. RESULTS AND DISCUSSION

Let us consider the angular distributions for the  $^{12}\text{C}(K^-, \pi^-)_{\Lambda}^{12}\text{C}$  reaction at  $p_K = 800$  MeV/c in the DWIA. Here we obtain the single-particle states for a neutron, using the Woods-Saxon potential [31] with a strength parameter of  $V_0^N = -64.8$  MeV, which is adjusted to reproduce the data of the charge radius of 2.46 fm [32]. For a  $\Lambda$ , we calculate the single-particle states, using the Woods-Saxon potential with  $V_0^\Lambda = -30.3$  MeV,  $a = 0.60$  fm,  $R = 2.58$  fm, and a spin-orbit strength of  $V_{ls}^\Lambda = 2$  MeV for  $A = 12$  [33,34], leading to the calculated energies of  $\varepsilon_\Lambda(0s_{1/2}) = -11.36$  MeV,  $\varepsilon_\Lambda(0p_{3/2}) = -0.60$  MeV, and  $\varepsilon_\Lambda(0p_{1/2}) = -0.32$  MeV. We perform the extended OFA for the  $K^-n \rightarrow \pi^- \Lambda$  reaction, using the elementary amplitudes analyzed by Gopal *et al.* [35], and we estimate the angular distributions for the  $^{12}\text{C}(K^-, \pi^-)_{\Lambda}^{12}\text{C}$  reaction according to Eq. (2).

#### A. In-medium $K^-n \rightarrow \pi^- \Lambda$ differential cross sections

Figure 3 shows the calculated results of the in-medium  $K^-n \rightarrow \pi^- \Lambda$  differential cross sections of  $\alpha|\bar{f}_{K^-n \rightarrow \pi^- \Lambda}|^2$  on the  $^{12}\text{C}$  target, together with the asymptotic momentum transfer  $q_{K\pi}$  in the  $^{12}\text{C}(K^-, \pi^-)_{\Lambda}^{12}\text{C}$  reaction, as a function of  $p_K$  in the laboratory frame. We find that the values of  $\alpha|\bar{f}_{K^-n \rightarrow \pi^- \Lambda}|^2$  obtained by the extended OFA are reduced in the region of  $p_K = 550\text{--}900$  MeV/c that corresponds to  $q_{K\pi} \lesssim 80$  MeV/c; the peak position is located at  $p_K \simeq 900$  MeV/c, which seems to shift upward in terms of the elementary cross sections in free space (FREE) [35] including the kinematical factor  $\alpha$ . These values of  $\alpha|\bar{f}_{K^-n \rightarrow \pi^- \Lambda}|^2$  may be simulated by the extended OFA using a constant of  $(q^2)^{1/2} \simeq 200$  MeV/c as an effective momentum transfer near the nuclear surface.

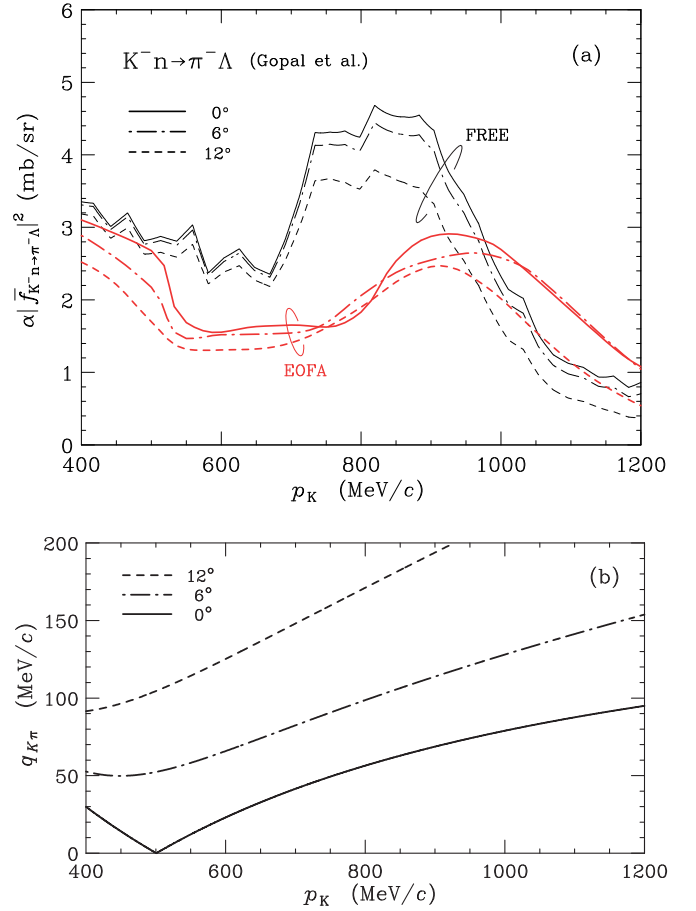


FIG. 3. (a) In-medium  $K^-n \rightarrow \pi^- \Lambda$  differential cross sections of  $\alpha|\bar{f}_{K^-n \rightarrow \pi^- \Lambda}|^2$  obtained by the extended OFA (EOFA) on the  $^{12}\text{C}$  target, together with the elementary cross sections in free space (FREE) including the kinematical factor  $\alpha$ . The amplitudes analyzed by Gopal *et al.* [35] are used. Solid, dot-dashed, and dashed curves denote the values of  $\alpha|\bar{f}_{K^-n \rightarrow \pi^- \Lambda}|^2$  for  $\theta_{\text{lab}} = 0^\circ, 6^\circ$ , and  $12^\circ$ , respectively. (b) The asymptotic momentum transfer  $q_{K\pi}$  in the  $^{12}\text{C}(K^-, \pi^-)_{\Lambda}^{12}\text{C}$  reaction, as a function of  $p_K$  in the laboratory frame.

We examine the behavior of  $\alpha|\bar{f}_{K^-n \rightarrow \pi^- \Lambda}|^2$  by the extended OFA, comparing it with that obtained by the SFA [11] on the  $^{12}\text{C}$  target at  $\theta_{\text{lab}} = 0^\circ$ , as shown in Fig. 4. We find that the absolute values of  $\alpha|\bar{f}_{K^-n \rightarrow \pi^- \Lambda}|^2$  by the SFA (FREE) are 1.8 (2.4) times larger than those by the extended OFA at 800 MeV/c at the forward direction angles; the values by the SFA agree with the results of  $\alpha|\langle f_L(0) \rangle|^2$  shown in Fig. 4 of Ref. [7]. Here we estimate the values by the SFA that includes the binding effects for a struck neutron via the  $^{12}\text{C}(K^-, \pi^-)_{\Lambda}^{12}\text{C}$  reaction (SFA+ $B_{\text{eff}}$ ) because the binding effects are not taken into account in the SFA. Such effects are roughly evaluated by a momentum shift  $\Delta p_K$  that is needed to populate a  $\Lambda$  hyperon from the  $0p_{3/2}$  neutron bound in  $^{12}\text{C}$ , supplying a separation energy of  $|\varepsilon_N(0p_{3/2})| \simeq (\Delta p_K)^2/2m_K$  where  $m_K$  is a mass of  $K^-$ . Thus, we have

$$\begin{aligned} \Delta p_K &= \sqrt{2m_K|\varepsilon_N(0p_{3/2})|} \\ &= \sqrt{2 \times 494 \times 19} \simeq 140 \text{ MeV/c}. \end{aligned} \quad (12)$$

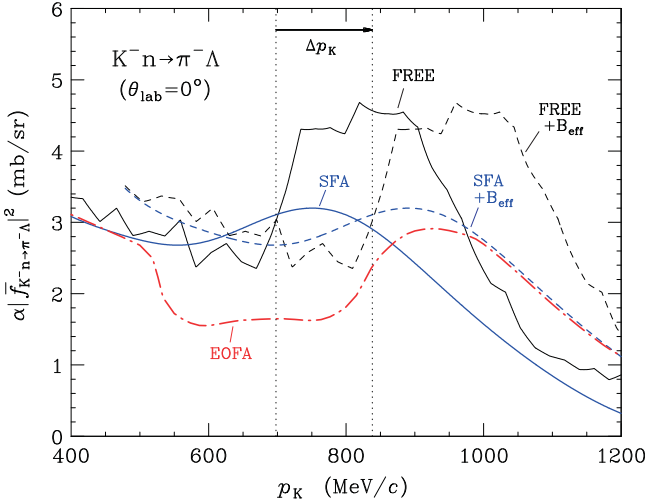


FIG. 4. Comparison of the calculated results of  $\alpha|\bar{f}_{K^-n \rightarrow \pi^- \Lambda}|^2$  obtained by the extended OFA (dot-dashed curve) with those obtained by the SFA and by the FREE on a  $^{12}\text{C}$  target at  $\theta_{\text{lab}} = 0^\circ$ . Solid and dashed curves denote the values of  $\alpha|\bar{f}_{K^-n \rightarrow \pi^- \Lambda}|^2$  without and with a 140-MeV/c momentum upward shift of  $\Delta p_K$  due to the binding effects ( $B_{\text{eff}}$ ), respectively.

In Fig. 4, we also draw the values of  $\alpha|\bar{f}_{K^-n \rightarrow \pi^- \Lambda}|^2$  by the SFA+ $B_{\text{eff}}$ , which are shifted upward by a 140-MeV/c momentum range of  $\Delta p_K$  when the binding effects are taken into account. We find that these values by the SFA+ $B_{\text{eff}}$  are nearly equal to those by the extended OFA at  $p_K \gtrsim 1000$  MeV/c because the extended OFA provides the binding effects automatically. On the other hand, the difference between the former and the latter gradually becomes bigger at  $p_K \lesssim 1000$  MeV/c due to the region of  $q^2/2\Delta m < \Delta\omega$ . For the FREE, we realize that the position of  $\alpha|\bar{f}_{K^-n \rightarrow \pi^- \Lambda}|^2$  should be shifted upward by the momentum range of  $\Delta p_K$  when the binding effects are taken into account (FREE+ $B_{\text{eff}}$ ), as seen in Fig. 4. Consequently, we show the validity of the extended OFA and the meaning of the binding effects necessary to make a good description for the  $K^-n \rightarrow \pi^- \Lambda$  differential cross sections at the forward direction angles.

Furthermore, we note that when the elementary  $K^-n \rightarrow \pi^- \Lambda$  amplitudes analyzed by Zhang *et al.* [36] are used, the calculated values of  $\alpha|\bar{f}_{K^-n \rightarrow \pi^- \Lambda}|^2$  in the extended OFA are very similar to those analyzed by Gopal *et al.* [35]. This situation is the same as that in the SFA. Therefore, we believe that the dependence of  $\alpha|\bar{f}_{K^-n \rightarrow \pi^- \Lambda}|^2$  on the elementary  $K^-n \rightarrow \pi^- \Lambda$  amplitudes is relatively small in the extended OFA and the SFA.

### B. Angular distributions for the $^{12}\text{C}(K^-, \pi^-)^{12}\text{C}$ reaction at 800 MeV/c

Now we estimate the angular distributions of the laboratory differential cross sections  $d\sigma/d\Omega_{\text{lab}}$  for  $^{12}\text{C}$  in the DWIA with the extended OFA. Figure 5 shows the calculated values of  $d\sigma/d\Omega_{\text{lab}}$  for  $1^-$ (g.s.) and for  $0^+$ ,  $2_1^+$ , and  $2_2^+$ (exc.) in  $^{12}\text{C}$ , together with the experimental data [3]. In Fig. 5(a), we display the calculated angular distributions for  $0^+$ (exc.)

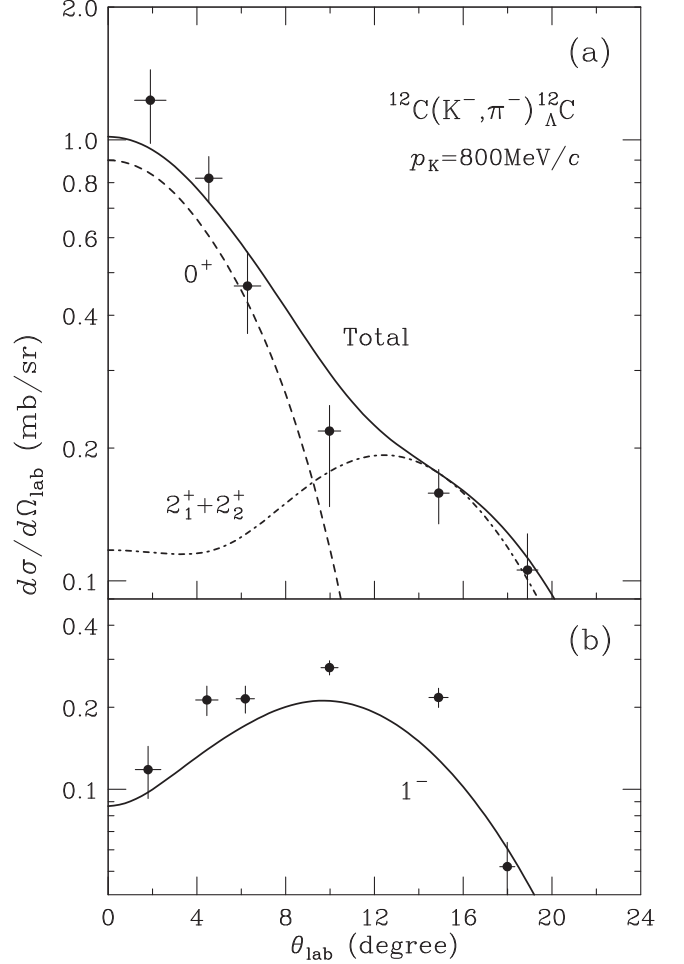


FIG. 5. Calculated angular distributions of the laboratory differential cross sections  $d\sigma/d\Omega_{\text{lab}}$  for (a) the  $0^+$ (exc.) and  $2_{1,2}^+$ (exc.) states, and for (b) the  $1^-$ (g.s.) state in  $^{12}\text{C}$  via the  $^{12}\text{C}(K^-, \pi^-)^{12}\text{C}$  reaction at  $p_K = 800$  MeV/c, together with the experimental data, as a function of the angle of  $\theta_{\text{lab}}$  in the laboratory frame. The calculated results are obtained in the DWIA with the extended OFA. The data are taken from Ref. [3].

and  $2_{1,2}^+$ (exc.), which have the  $[(0p_{3/2,1/2})_\Lambda(0p_{3/2})_n^{-1}]_{0^+}$  and  $[(0p_{3/2,1/2})_\Lambda(0p_{3/2})_n^{-1}]_{2^+}$  configurations, respectively. These  $\Lambda$  excited states are located near the  $\Lambda$ - $^{11}\text{C}$  threshold at  $B_\Lambda^{\text{cal}}(0^+, 2_{1,2}^+) = 0.32\text{--}0.60$  MeV. We find that the shape and magnitude of the calculated sum values of  $0^+$ ,  $2_1^+$ , and  $2_2^+$ (exc.) in the extended OFA are in good agreement with those of the data in the whole angles of  $\theta_{\text{lab}} = 0^\circ\text{--}20^\circ$ . Note that the renormalization of these calculated cross sections by a factor is not necessary to reproduce the magnitude of the data, in contrast with several results estimated by earlier DWIA calculations [6,7,9,10]. In Fig. 5(b), we display the calculated angular distribution for  $1^-$ (g.s.) having the  $[(0s_{1/2})_\Lambda(0p_{3/2})_n^{-1}]_{1^-}$  configuration. We find that the shape of the calculated value of  $1^-$ (g.s.) agrees with that observed in the data, whereas its magnitude rather underestimates at  $4^\circ < \theta_{\text{lab}} < 16^\circ$ , which is about 20% smaller than that of the data. This discrepancy may be because more sophisticated treatments of nuclear wave functions are needed for more

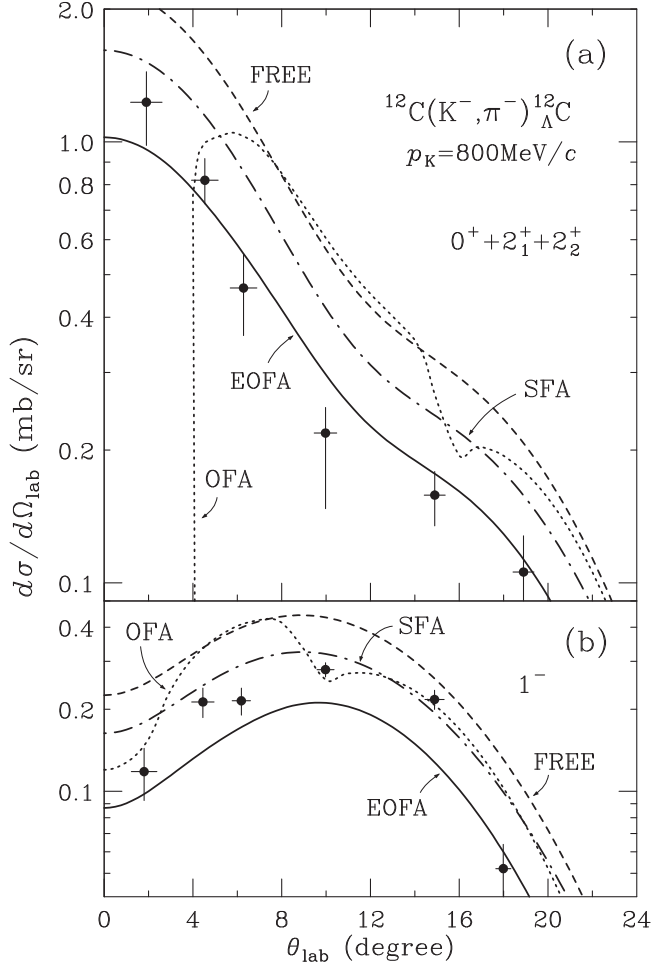


FIG. 6. Comparison with the angular distributions estimated in several DWIA calculations. The calculated results of  $d\sigma/d\Omega_{\text{lab}}$  are shown for (a)  $0^+ + 2_1^+ + 2_2^+$ (exc.) and (b)  $1^-$ (g.s.) in  $^{12}\text{C}$  via the  $^{12}\text{C}(K^-, \pi^-)^{12}\text{C}$  reaction at  $p_K = 800 \text{ MeV}/c$ . Solid curves denote our results of the extended OFA (EOFA). Dotted, dot-dashed, and dashed curves denote the values of the OFA omitting the effect of the local momentum transfer, the SFA, and the FREE, respectively. The data are taken from Ref. [3].

detailed comparison, e.g., a configuration mixing [6,10], a 2p-2h admixture, and other many-body effects beyond single-particle descriptions.

Figure 6 shows the comparison of our results for the extended OFA with those for the “standard” DWIA calculations. The quantities  $\bar{f}_{K^-n \rightarrow \pi^- \Lambda}$  are estimated in the DWIA with the elementary amplitude in free space (FREE) [6] and with the SFA amplitude [7,11]. We confirm that the magnitude of  $d\sigma/d\Omega_{\text{lab}}$  with the FREE amplitude is 2.1 times as large as that of the data, and the magnitude with the SFA amplitude is still larger than that of the data by a factor of 1.6, as discussed in Ref. [6]. Therefore, it seems that the estimations of the standard DWIA are insufficient to explain the data, whereas these shapes of  $d\sigma/d\Omega_{\text{lab}}$  moderately agree with those of the data [6,7,9,10].

In the case of the OFA omitting the effect of the local momentum transfers, we confirm that the shape and magnitude of  $d\sigma/d\Omega_{\text{lab}}$  hardly agree with those of the data; no

$\Lambda$  in  $(0p_{3/2})_{\Lambda}$  is populated at  $\theta_{\text{lab}} \lesssim 4^\circ$  due to  $q^2/2\Delta m < \Delta\omega$  for  $q = q_{K\pi} \simeq 55\text{--}80 \text{ MeV}/c$ , whereas a  $\Lambda$  in  $(0s_{1/2})_{\Lambda}$  is populated due to  $q^2/2\Delta m \gtrsim \Delta\omega$ . As seen in Fig. 6(b), its shape behaves remarkably owing to the on-energy-shell condition of  $(p_N^*, \theta_N^*)$  determined from Eq. (10) in the OFA that accompanies a Fermi averaging over a narrow width of  $2p_N^*q/m_{\Lambda}$ . This result indicates that the OFA with only  $q_{K\pi}$  does not work in the near-recoilless reaction having  $q \lesssim 80 \text{ MeV}/c$  because of the unavoidable difficulty of  $q^2/2\Delta m < \Delta\omega$  or  $q^2/2\Delta m \approx \Delta\omega$ . This difficulty is overcome by the extended OFA providing the effect of the local momentum transfer; the calculated shape and magnitude of  $d\sigma/d\Omega_{\text{lab}}$  for  $0^+ + 2_1^+ + 2_2^+$ (exc.) and  $1^-$ (g.s.) can explain those of the data without a renormalization factor quantitatively.

Consequently, we show that the effect of the local momenta generated by the semiclassical distorted waves for the mesons overcomes severe difficulties of the previous OFA procedure in the near-recoilless reactions such as  $(K^-, \pi^-)$ . This result may imply the validity of the semiclassical picture of the localized on-energy-shell collisions by distorted waves for the mesons.

On the other hand, it should be noticed that the endothermic  $(\pi^+, K^+)$  reaction on nuclei satisfies the condition of  $q(r) \lesssim q_{\pi K}$ , where  $q_{\pi K}$  is an asymptotic momentum transfer having  $q_{\pi K} \simeq 300\text{--}500 \text{ MeV}/c$ . There is no difficulty in the OFA without handling the local momentum transfer because the effect of the local momentum transfer is rather small in the nuclear  $(\pi^+, K^+)$  reaction. Therefore, we recognize that the OFA procedure obeying the asymptotic  $q_{\pi K}$  works well in the  $(\pi^+, K^+)$  reaction [16].

#### IV. SUMMARY AND CONCLUSION

We proposed to extend the OFA procedure theoretically in order to calculate an in-medium  $K^-n \rightarrow \pi^- \Lambda$  amplitude of  $\bar{f}_{K^-n \rightarrow \pi^- \Lambda}$  for the exothermic  $(K^-, \pi^-)$  reaction on nuclei in the framework of the DWIA, taking into account the local momentum transfer generated by semiclassical distorted waves for  $K^-$  and  $\pi^-$ . Applying the extended OFA procedure, we estimated the angular distributions for the  $^{12}\text{C}(K^-, \pi^-)^{12}\text{C}$  reaction at  $p_K = 800 \text{ MeV}/c$  under the near-recoilless condition of  $q \lesssim 80 \text{ MeV}/c$ , and we showed that the calculated angular distributions are in good agreement with those of the data.

In conclusion, the extended OFA procedure provides the effect of the local momentum transfer generated by the meson distorted waves. This extension is a successful prescription making it possible to describe the reaction cross sections in the near-recoilless reactions such as  $(K^-, \pi^-)$  in our framework. This work may be a basis for studies clarifying the mechanism of the hadron production reactions on nuclei, and extracting the properties of a hadron-nucleus potential from the experimental data [37].

#### ACKNOWLEDGMENTS

The authors thank Professor M. Kawai for many valuable discussions and comments. This work was supported by Grants-in-Aid for Scientific Research (KAKENHI) from the Japan Society for the Promotion of Science: Scientific Research (C) (Grant No. JP20K03954).

- [1] W. Brückner *et al.*, *Phys. Lett. B* **62**, 481 (1976).
- [2] W. Brückner *et al.* (Heidelberg-Saclay-Strasbourg Collaboration), *Phys. Lett. B* **79**, 157 (1978).
- [3] R. E. Chrien *et al.*, *Phys. Lett. B* **89**, 31 (1979).
- [4] M. I. Podgoretsky, *Sov. Phys. JETP* **44**, 695 (1963); H. Feshbach and A. Kerman, in *Preludes in Theoretical Physics*, edited by A. De-Shalit, H. Feshbach, and L. Van Hove (North-Holland, Amsterdam, 1966), p. 260.
- [5] A. K. Kerman and H. J. Lipkin, *Ann. Phys.* **66**, 738 (1971).
- [6] C. B. Dover, A. Gal, G. E. Walker, and R. H. Dalitz, *Phys. Lett. B* **89**, 26 (1979).
- [7] E. H. Auerbach, A. J. Baltz, C. B. Dover, A. Gal, S. H. Kahana, L. Ludeking, and D. J. Millener, *Ann. Phys.* **148**, 381 (1983).
- [8] J. Žofka, M. Sotona, and V. N. Fetisov, *Nucl. Phys. A* **431**, 603 (1984).
- [9] H. Bandō, T. Motoba, and J. Žofka, *Int. J. Mod. Phys. A* **05**, 4021 (1990).
- [10] K. Itonaga, T. Motoba, and M. Sotona, *Prog. Theor. Phys. Suppl.* **117**, 17 (1994).
- [11] A. S. Rosenthal and F. Tabakin, *Phys. Rev. C* **22**, 711 (1980).
- [12] T. Nagae, in *Proceedings of the 14th Asia-Pacific Physics Conference*, edited by T.-Y. Tou, J. Yokoyama, R. A. Shukor, K. Tanaka, H. J. Choi, R. Matsumoto, O.-H. Chin, J. H. Chin, and K. Ratnavelu, AIP Conf. Proc. No. 2319 (AIP, New York, 2021), p. 020002.
- [13] T. Harada and Y. Hirabayashi, *Nucl. Phys. A* **759**, 143 (2005).
- [14] T. Harada and Y. Hirabayashi, *Nucl. Phys. A* **767**, 206 (2006).
- [15] T. Harada, R. Honda, and Y. Hirabayashi, *Phys. Rev. C* **97**, 024601 (2018).
- [16] T. Harada and Y. Hirabayashi, *Nucl. Phys. A* **744**, 323 (2004).
- [17] T. Harada and Y. Hirabayashi, *Phys. Rev. C* **103**, 024605 (2021).
- [18] M. Kohno, Y. Fujiwara, Y. Watanabe, K. Ogata, and M. Kawai, *Phys. Rev. C* **74**, 064613 (2006).
- [19] S. Hashimoto, M. Kohno, K. Ogata, and M. Kawai, *Prog. Theor. Phys.* **119**, 1005 (2008).
- [20] Y. L. Luo and M. Kawai, *Phys. Rev. C* **43**, 2367 (1991).
- [21] M. Kawai, *Prog. Theor. Phys.* **27**, 155 (1962).
- [22] J. Hüfner, S. Y. Lee, and H. A. Weidenmüller, *Nucl. Phys. A* **234**, 429 (1974).
- [23] C. B. Dover, L. Ludeking, and G. E. Walker, *Phys. Rev. C* **22**, 2073 (1980).
- [24] C. B. Dover and A. Gal, *Ann. Phys.* **146**, 309 (1983).
- [25] R. A. Eisenstein and A. Miller, *Comput. Phys. Commun.* **8**, 130 (1974).
- [26] D. Marlow, P. D. Barnes, N. J. Colella, S. A. Dytman, R. A. Eisenstein, R. Grace, F. Takeuchi, W. R. Wharton, S. Bart, D. Hancock, R. Hackenberg, E. Hungerford, W. Mayes, L. Pinsky, T. Williams, R. Chrien, H. Palevsky, and R. Sutter, *Phys. Rev. C* **25**, 2619 (1982).
- [27] T. Takahashi, H. Sakaguchi, K. Aoki, T. Hasegawa, O. Hashimoto, T. Nagae, M. Sekimoto, A. Ohkusu, H. Bhang, H. Yu, and Y. Gavrilo, *Phys. Rev. C* **51**, 2542 (1995).
- [28] A. Matsuyama and K. Yazaki, *Nucl. Phys. A* **477**, 673 (1988).
- [29] H. De Vries, C. W. De Jager, and C. De Vries, *At. Data Nucl. Data Tables* **36**, 495 (1987).
- [30] S. A. Gurvitz, *Phys. Rev. C* **33**, 422 (1986).
- [31] A. Bohr and M. Mottelson, *Nuclear Structure* (Benjamin, New York, 1969), Vol. 1, p. 238.
- [32] G. Jacob and T. A. J. Maris, *Rev. Mod. Phys.* **38**, 121 (1966).
- [33] D. J. Millener, C. B. Dover, and A. Gal, *Phys. Rev. C* **38**, 2700 (1988).
- [34] A. Gal, E. V. Hungerford, and D. J. Millener, *Rev. Mod. Phys.* **88**, 035004 (2016).
- [35] G. P. Gopal *et al.*, *Nucl. Phys. B* **119**, 362 (1977).
- [36] H. Zhang, J. Tulpan, M. Shrestha, and D. M. Manley, *Phys. Rev. C* **88**, 035204 (2013).
- [37] A. Cieplý, E. Friedman, A. Gal, and V. Krejcirík, *Phys. Lett. B* **698**, 226 (2011).